Tissue heterogeneity is associated with phenotypic but not genomic diversity in *Wolbachia* endosymbionts

Romain Pigeault[1*], Yann Dussert[1], Raphaël Jorge[3,4], Theo Ulve[1], Marie Panza[1], Maryline Raimond[1], Carine Delaunay[1], Willy Aucher[1], Thierry Berges[1], David Ogereau[5], Bouziane Moumen[1], Jean Peccoud[1†], Richard Cordaux[5†]

[1] Université de Poitiers, CNRS, EBI, UMR 7267, Poitiers, France

[2] Génomique Métabolique, Genoscope, Institut François Jacob, CEA, CNRS, Univ Evry, Université Paris-Saclay, Evry, 91057, France

[3] Université Lyon 1, CNRS, VetAgroSup, Laboratoire de Biométrie et Biologie Evolutive, UMR 5558, Villeurbanne, France

[4] INSA Lyon, INRAE, Biologie fonctionnelle, insectes et interactions, UMR203, Villeurbanne, France

[5] Université Paris-Saclay, CNRS, IRD, UMR Évolution Génomes Comportement Écologie, 91190 Gif-sur-Yvette, France

ORCID :

Romain Pigeault: 0000-0002-8011-4600

Yann Dussert: 0000-0003-1900-7715

David Ogereau : 0000-0002-4496-3007

Bouziane Moumen: 0000-0002-1789-6160

Jean Peccoud: 0000-0002-3356-7869

Richard Cordaux: 0000-0003-4997-735X

*Corresponding author: **Romain Pigeault -** romain.pigeault@univ-poitiers.fr

[†] Jean Peccoud and Richard Cordaux share senior authorship

Running Head: *Wolbachia* within-host diversity

Abstract

The mechanisms underlying within-host diversification in parasite populations are poorly understood. Yet, phenotypic and genotypic variation in parasites can shape their evolutionary trajectories and have important epidemiological consequences. Our aim was to determine whether the constraints associated with infecting different host tissues lead to the emergence and coexistence of multiple parasite sub-populations with distinct phenotypes. We tested this hypothesis using the most widespread bacterial endosymbiont, *Wolbachia*. We injected *Wolbachia* bacteria isolated from three tissues of the common pill-bug (*Armadillidium vulgare*) into uninfected individuals and monitored the growth rate and virulence of each bacterial sub-population in the new hosts. Our results highlight that within-host tissue heterogeneity leads to diverse *Wolbachia* phenotypes. High-depth genome re-resequencing of *Wolbachia* sub-populations revealed that this polymorphism was not due to genomic variation but was more likely a result of phenotypic plasticity. Indeed, we found no recurrent tissue-specific genomic variation among infected individuals. Our single nucleotide polymorphism (SNP) filtration pipeline, developed to ensure SNP validity, detected only one substitution. This *Wolbachia* variant, observed in one female, was present in all three bacterial sub-populations, with frequencies ranging from 24% to 58% depending on the tissue. Overall, our results support the stability of the *Wolbachia* genome with respect to the rarity of point mutations, in agreement with reports from other symbiotic systems. From a methodological perspective, our study highlights the need for considerable caution when detecting variants in endosymbiont populations, as our conservative approach led us to exclude more than 99.5% of the initially called variants.

Keywords: adaptation, acclimation, feminizing *Wolbachia*, infection dynamics, subpopulation, tissue tropism, variant calling, within-host evolution

50 # 1. Introduction

51 Among the many factors that influence species richness and community structure,
52 environmental heterogeneity is generally considered to be a particularly important driver
53 (Ben-Hur & Kadmon, 2020; Stein et al., 2014; Stein & Kreft, 2015). Since heterogeneous
54 environments offer a variety of ecological niches and refuges from adverse conditions, species
55 richness and persistence should increase with greater spatial heterogeneity (Ben-Hur &
56 Kadmon, 2020; Burnett et al., 1998; Stein et al., 2014; Yang et al., 2015). Environmental
57 heterogeneity also promotes genetic and phenotypic diversity within species through
58 diversifying selection (Houle et al., 2020; B.-H. Huang et al., 2017; Mcdonald & Ayala, 1974;
59 Rainey & Travisano, 1998), which may underpin local adaptations (Y. Huang et al., 2016; Qian
60 et al., 2024; Trevail et al., 2021; van Houte et al., 2021). However, most studies that
61 investigated relationships between environmental heterogeneity and diversity have focused
62 on free-living species (e.g., (Langenheder & Lindström, 2019; Stein & Kreft, 2015)). The
63 relationship between environmental heterogeneity and both endoparasites species diversity
64 and phenotypic variability remains underexplored.

65 For endoparasites, environmental heterogeneity can exist both within individual hosts and
66 across different hosts. Variation among individuals within host population is known to shape
67 parasite evolution (Johnson et al., 2016; Regoes et al., 2000; White et al., 2020), driving rapid
68 diversification (Johnson et al., 2016; Kamiya et al., 2014). However, a single host individual is
69 treated by most theoretical and empirical studies on endoparasite evolution as a
70 homogeneous environment – a single population of target cells without any structure –
71 neglecting heterogeneities in cell type, immune response, nutrient supply or microbiota
72 composition. Yet, several parasites exploit a heterogeneous environment composed of

73 different biological tissues and fluids which form a spatially structured fitness landscape for
74 the parasite. Successful colonization of different microenvironments, with their contrasted
75 constraints, may involve the expression or selection of different parasitic phenotypes leading
76 to within-host differentiation into several sub-populations (Didelot et al., 2016). This
77 phenotypic variability can reflect phenotypic plasticity (e.g., expression plasticity,
78 (Wernegreen & Wheeler, 2009), selection of genetic variants initially present in the inoculum
79 (Chrostek & Teixeira, 2018) or of new variants arising from spontaneous mutations (Ailloud et
80 al., 2019).

81 The co-occurrence of polymorphic sub-populations of parasites in different tissues or
82 cell types has been described in several biological models. RNA viruses (e.g., plum pox virus,
83 influenza, SARS-CoV-2, poliovirus) may display genetic diversity within single infected hosts,
84 and co-existing viral variants may evolve differently in distinct cell types (Gupta et al., 2022;
85 Jridi et al., 2006; Xiao et al., 2017). The ability of some RNA viruses to adapt to tissue-specific
86 innate immune microenvironments may actually be critical for establishing robust infections
87 (Xiao et al., 2017). Gastric biopsies from multiple stomach regions of *Helicobacter pylori*-
88 infected hosts showed location-specific evolution of the bacteria, suggesting the existence of
89 structured niches with distinct selective pressures within the stomach (Ailloud et al., 2019). In
90 other cases, such as *Pseudomonas aeruginosa* or *Mycobacterium tuberculosis* chronic
91 infections, the emergence of polymorphic sub-populations seems to be driven by tissue-
92 specific adaptation (Jorth et al., 2015; Lieberman et al., 2016). Some within-host parasite sub-
93 populations may constitute a reservoir from which new virulent variants can emerge (Bessière
94 & Volmer, 2021), and which can delay clearance of parasite infection by the host immune
95 system or drugs (Avettand-Fenoel et al., 2011; Clement et al., 2005; Obaldia et al., 2018).
96 Understanding the evolutionary forces and mechanisms at the origin of within-host parasite

97 diversity is essential, yet it is rarely studied. Descriptive studies (e.g., long-term ambulatory
98 monitoring of chronically infected patients) cannot trace the divergence of variants found
99 within a host and cannot identify the drivers of their diversification without controlling or
100 assessing the composition of the infectious inoculum and ensuring the absence of subsequent
101 infections. For this purpose, vertically transmitted parasites are particularly useful, as their
102 transmission mode ensures the common origin of all within-host parasite sub-populations.

103 Among the most widespread vertically transmitted endosymbionts in animals is
104 *Wolbachia pipientis*. This primarily maternally transmitted intracellular alpha-
105 proteobacterium is widely distributed among arthropods and has been extensively studied
106 with respect to its peculiar effects on its hosts (Kaur et al., 2021; LePage & Bordenstein, 2013).
107 *Wolbachia* manipulates host reproduction in various ways, including the feminization of
108 chromosomal male embryos, parthenogenesis, male killing, and sperm–egg incompatibility
109 (Werren et al., 2008)). This endosymbiont can also have positive or negative effects on other
110 aspects of the host's life cycle (e.g., immunity, senescence) and influence the evolution of the
111 host genome through horizontal gene transfer (Cordaux & Gilbert, 2017; Depeux et al., 2024;
112 Sicard et al., 2014). The diversity of effects of *Wolbachia* on its hosts certainly relates to its
113 wide distribution within infected individuals (Sicard et al., 2014). In addition to colonizing the
114 female germline, ensuring vertical transmission, *Wolbachia* has indeed been observed in all
115 major tissues (e.g., nerve chain, immune and digestive compartments, (Pietri et al., 2016)) of
116 many arthropod species. The presence of vertically transmitted endosymbionts in somatic
117 tissues may seem paradoxical, especially considering that systemic infection can decrease host
118 fitness. Given this disadvantage (i.e., fitness alignment), these extensive somatic localizations
119 must somehow benefit the parasite. Localization of *Wolbachia* in somatic tissues could
120 influence host biology in such a way that favours its vertical and, possibly, horizontal

121 transmission. However, the ability of the bacteria to colonize and establish in different tissular
122 microenvironments could involve the expression or selection of different phenotypes.

123 To investigate this hypothesis, we assessed the relationship between tissue
124 environment heterogeneity and phenotype variability in the *w*VulC *Wolbachia* strain, which
125 infects the common pill-bug *Armadillidium vulgare* (Cordaux et al., 2004). We focused on three
126 naturally infected tissues, which we selected for their physiological characteristics and the
127 benefits that *Wolbachia* could gain by colonizing them: (i) gonads, which are a prime target
128 for vertical transmission, (ii) haemocytes, as these circulating immune cells could contribute
129 to spread *Wolbachia* to different host tissues and may facilitate its horizontal transmission
130 (Braquart-Varnier et al., 2015), and (iii) the nerve chain, as the localization of *Wolbachia* in the
131 brain and nerve chord could induce adaptive modifications of host behaviour (Bi & Wang,
132 2020; Templé & Richard, 2015). We hypothesized that the main phenotypic variation between
133 bacteria sub-populations colonizing these tissues pertained to their replication rate. A high
134 replication rate in vital tissues, such as the nerve chain, could disrupt tissue structure and
135 reduce host lifespan (Le Clec'h et al., 2012; Strunov & Kiseleva, 2016). Thus, we expected
136 *Wolbachia* populations from the host nerve system to show lower replication rates than those
137 from the other tissues. We tested this hypothesis by injecting *Wolbachia* extracted from the
138 three tissue types into uninfected *A. vulgare* individuals, and by monitoring their growth rates
139 in their new hosts. We then tested whether *Wolbachia* sub-populations were adapted and not
140 merely acclimated to their tissue types. In this case, we expected to find recurrent tissue-
141 specific genomic variation among infected individuals. We tested this prediction by
142 sequencing the whole genomes of focal bacterial sub-populations.

143 # 2. Materials and Methods

144 ## 2.1 Biological models

145 All *A. vulgare* individuals used in this experiment were reared as previously described (Sicard
146 et al., 2010). Given that the *Wolbachia* strain used in this study is feminizing, all the individuals
147 used were females. As *Wolbachia* is not cultivable, phenotyping sub-populations requires
148 trans-infection of an uninfected host with bacterial isolates from naturally infected animals.
149 For this purpose, we used a common pill-bug source line (WXw) infected by the *w*VulC
150 *Wolbachia* strain (source individuals) and an uninfected recipient line (WXa, recipient
151 individuals) into which we have injected bacteria. The two laboratory lines came from the
152 same original population sampled in Helsingør (Denmark).

153 ## 2.2 Experimental infection

154 To characterize the phenotype of the different *Wolbachia* sub-populations associated to three
155 different tissues of their native host, five batches of trans-infection were carried out. Three
156 batches (i.e., three biological replicates) were used to monitor early infection dynamics within
157 the recipient host (day 0 to day 60 post-infection, trans-infection experiment 1), and two
158 batches were used to estimate bacterial persistence in tissues (i.e., two biological replicates,
159 day 200 post-infection, trans-infection experiment 2). For each batch, one tissue suspension
160 was prepared from each of the following tissues: haemolymph, ovaries and nerve chain.
161 Tissues were collected from five source females from the WXw line (infection status previously
162 validated by quantitative PCR, see section 2.4). For each suspension, tissues were crushed in
163 1 mL of Ringer solution (1.4 mM CaCl2, 2.4 mM HNaCO3, 2 mM KCl, 0.4 M NaCl) for
164 haemolymph and 2 mL for ovaries and nerve chain. The resulting suspension was filtered
165 through a 1.2 µm pore membrane to remove cell debris and host cell nuclei. A prior

166 experiment conducted on 15 females from the source line (WXw) allowed us to highlight that
167 the number of bacteria per ng of DNA differed between the three target tissues (see **Fig. S1** in
168 appendix 1). Therefore, the filtered solutions were diluted in Ringer solution to adjust the final
169 concentration of bacteria at 2500 ± 300 cells/µL for the trans-infection batches used to
170 describe *Wolbachia* infection dynamics, and at 1282 ± 205 cells/µL for the two batches made
171 to investigate bacterial persistence 200 days after injection. The variation in *Wolbachia*
172 concentration between the two experiments stems from their differing timing, with the first
173 conducted in January and the second in April. Since *Wolbachia* concentration (number/ng of
174 DNA) can fluctuate based on host size and, consequently, age, this resulted in slight
175 differences in *Wolbachia* concentration between the two trans-infection experiments.
176 Another prior experiment showed that the proportion of live bacteria in the different filtered
177 tissue solutions was similar (LRT = 4.0279, p = 0.1335, proportion of live *Wolbachia* ± 95%CI,
178 haemolymph = 0.815 ± 0.017, nervous chain = 0.875 ± 0.014, ovaries = 0.862 ± 0.037, see
179 appendix 1 for a detailed protocol).

180 One µL of each filtrate was injected using a thin glass needle into the general cavity of
181 each recipient individual through a small hole pierced at its posterior part. Each tissue filtrate
182 from the three trans-infection batches used to study *Wolbachia* infection dynamics (trans-
183 infection experiment 1) was injected into 21 recipient females of the WXa line, resulting in a
184 total of 63 females transinfected per tissue filtrate. Then, on days 20, 40 and 60 post-injection,
185 6-7 recipient females per trans-infection batch were randomly selected to quantify *Wolbachia*
186 in the focal tissues (see section 2.4). To study bacterial persistence in recipient host tissues
187 (trans-infection experiment 2), 10 females were injected with each tissue filtrate for each of
188 the two trans-infection batches. Two hundred days post-injection, all surviving females were
189 dissected to quantify *Wolbachia* in the three focal tissues (see section 2.4). For each trans-

190 infection batch, control groups were created using the same protocol, but with female sources
191 originating from the WXa line.

192 ## 2.3 Mortality monitoring

193 The effect of *Wolbachia* injection on pill-bug mortality was monitored every 10 days as part
194 of the study of the influence of *Wolbachia* tissue origin on the dynamics of early infection
195 within the recipient host (trans-infection experiment 1), and every 15-25 days as part of the
196 study of *Wolbachia* tissue origin on the persistence of the bacterium in tissues (trans-infection
197 experiment 2). When individuals were harvested during the experiment to quantify
198 *Wolbachia*, they were censored for the survival analysis (see section 2.9).

199 ## 2.4 Quantification of *Wolbachia* in source and recipient host's tissues

200 To compare *Wolbachia* density in different tissues of source line and recipient hosts, total DNA
201 was extracted from the haemolymph, nerve chain and ovaries of individuals using standard
202 protocols (Qiagen DNeasy 96 Blood & Tissue kit). For each sample, the purity of the extracted
203 DNA (OD 260/280 nm and 260/230 nm ratios) was measured using a Nanodrop 1000
204 spectrophotometer (Thermofisher). To quantify *Wolbachia* load, we developed a fluorescent
205 probe-based quantitative PCR (qPCR) approach amplifying a *Wolbachia* locus and a reference
206 host nuclear locus in the same reaction. We used primers wsp208f (5'- TGG-TGC-AGC-ATT-
207 TAC-TCC-AG-3') and wsp413r (5'-TCG-CTT-GAT-AAG-CAA-AAC-CA-3') targeting the *Wolbachia*
208 protein surface gene (*wsp*, (W. L. Le Clec'h et al., 2012)) and we designed primers amplifying
209 a portion of the single-copy nuclear gene encoding the mitochondrial leucine-tRNA ligase of
210 *A. vulgare*: TLeuF (5'- TGT-ACA-CAT-CGA-GCA-GCA-AG-3') and TLeuR (5'- AAA-GAG-GAG-CGG-
211 AGA-GTT-TCA-G-3') (Durand et al., 2023). The *Wolbachia wsp* double-dye probe (5'-TTG-CAG-
212 ACA-GTG-TGA-CAG-CGT-T-3') was labelled with Hexachlorofluorescein (HEX) as a reporter at
213 the 5' end and Black Hole Quencher 1 (BHQ-1) at the 3' end. *A. vulgare* TLeu probe (5'-ACG-

214 AAG-TTC-GCC-CTG-TTC-TGG-A-3') was labelled with 6-carboxy-fluorescein (FAM) as a reporter
215 and BHQ-1 as a quencher. The qPCR reactions were performed using Roche LIGHTCYCLER 480
216 with the following program: 2 min at 50°C, 10 min at 95°C and 45 cycles, 15 s at 95°C, and 1
217 min at 60°C. For each sample, two independent technical replicates were carried out and the
218 mean cycle-threshold value was calculated. *Wolbachia* load was then calculated relative to
219 the reference gene (TLeu) using the delate CP method: $2^{-(CP(wsp) - CP(TLeu))}$.

220 ## 2.5 Genome assembly of *Wolbachia w*VulC

221 To study the within-host genetic diversity of *Wolbachia*, we first assembled the genome of the
222 *w*VulC *Wolbachia* strain from the WXw line. Three female individuals were used for Oxford
223 Nanopore Technologies (ONT) long-read sequencing and one for Illumina short-read
224 sequencing. Total DNA from haemolymph, nerve chain and ovaries of each female was
225 extracted using standard protocols (DNA used for ONT sequencing: Macherey-Nagel
226 NucleoBond HMW DNA kit, DNA used for Illumina sequencing: Qiagen DNeasy 96 Blood &
227 Tissue kit). The long-read sequencing library was prepared using the SQK-LSK109 Ligation
228 Sequencing Kit (ONT) and sequenced with an R9.4.1 flow cell on a MinION Mk1B (ONT). Reads
229 were basecalled with Guppy 6.3.8 (RRID:SCR_023196) using the SUP model. The short-read
230 library was prepared using the TruSeq Nano DNA Library Prep kit (Illumina) and sequenced on
231 a HiSeq X (Illumina, paired-end 2 × 150 bp).

232 ONT adapters were first trimmed with porechop 0.2.4
233 (https://github.com/rrwick/Porechop), and reads were filtered using NanoFilt 2.7.1 (minimum
234 average quality: 7, minimum length: 1000 bp) implemented in NanoPack (De Coster et al.,
235 2018). Reads were then assembled with Flye 2.8.3 (Kolmogorov et al., 2019) using default
236 parameters. The entire assembly was first polished with the ONT reads using medaka 1.7
237 (https://github.com/nanoporetech/medaka, r941_min_fast_g507 model, 2 rounds). For

238 assembly polishing using short reads, Illumina reads were mapped onto the assembly with
239 bwa-mem2 2.2.1 (Vasimuddin et al., 2019) and used for further polishing with Polypolish 0.4.3
240 (Wick & Holt, 2022). This step was carried out twice. The largest assembled contig was
241 reported detected as circular by the Flye assembler and had the expected length (~1.6 Mb) of
242 the *w*VulC *Wolbachia* genome. We aligned this contig against a previous version of the
243 genome (GenBank accession: ALWU00000000.1) with nucmer in MUMmer 4.0.0rc1 (Marçais
244 et al., 2018), confirming that the contig corresponded to the *w*VulC strain. After mapping the
245 short reads for a third time onto this contig, short variants were called with Freebayes 1.3.1
246 (Garrison & Marth, 2012). Variants were then visually reviewed using the IGV genome browser
247 (version 2.14.0) (Robinson et al., 2017). Eight of them, corresponding to errors, were kept. We
248 corrected the genome sequence with these eight variants using the consensus command in
249 BCFtools 1.17 (Danecek et al., 2021). Following the recommendations of Ioannidis (Ioannidis
250 et al., 2007), the genome sequence was rotated to start at the *hemE* gene using the fixstart
251 command of Circlator 1.5.5 (Hunt et al., 2015) . The genome was annotated with the NCBI
252 Prokaryotic Genome Annotation Pipeline (PGAP) 2022-12-13.build6494 (Haft et al., 2024; Li et
253 al., 2021; Tatusova et al., 2016). A search of Insertion Sequence (IS) elements was carried out
254 with digIS v1.2 (Puterová & Martínek, 2021). Additionally, bacteriophage-derived regions were
255 detected using PHASTEST (Wishart et al., 2023). Results of these annotations were plotted
256 with Circos v0.69-9 (Krzywinski et al., 2009). The completeness of the genome and the gene
257 annotation was assessed using BUSCO 5.3.2 (Manni et al., 2021) using the rickettsiales_odb10
258 dataset.

259 ## 2.6 Whole-genome resequencing and variant calling

260 Three *A. vulgare* females from the WXw line were used to study the genetic diversity of the
261 different *Wolbachia* sub-populations associated with the nerve chain, ovaries and

262 haemolymph. Two of these females were sisters (names: F1_2015 & F2_2015). The matriline
263 of the third one (F_1999) diverged from the matriline of the sisters for 18 generations (i.e., 18
264 years). Females were dissected and their tissues isolated individually. Total DNA of each
265 biological sample was extracted using the Qiagen DNeasy 96 Blood & Tissue kit. DNA purity
266 and quantity were measured as described above. The haemolymph of two females could not
267 be sequenced because it did not yield enough DNA. DNA libraries were prepared using the
268 TruSeq Nano DNA Library Prep kit and sequenced on the Illumina HiSeq 2000 platform to
269 generate 2×150 bp reads, by Genoscreen (Lille, France). Read quality was assessed with
270 FastQC 0.11.9 (http://www.bioinformatics.babraham.ac.uk/projects/fastqc). Fastp 0.23.0
271 (Chen et al., 2018) was used to remove adapter contamination and systematic base calling
272 errors. To mitigate misalignments of reads originating from the host genome, notably from
273 *Wolbachia*-derived nuclear insertions (Chebbi et al., 2019; Leclercq et al., 2016), reads were
274 aligned using bwa-mem2 (Vasimuddin et al., 2019) against a reference including our *w*VulC
275 genome assembly, the assembly of the partial mitochondrial genome of *A. vulgare* (GenBank
276 accession number: MF187614.1, (Peccoud et al., 2017)) and the genome assembly of *A.*
277 *vulgare* (accession number: GCA_004104545.1, (Chebbi et al., 2019)). PCR duplicates were
278 marked with samtools markdup (v1.14). Read coverage along the *w*VulC genome was
279 computed for each sample for adjacent 5 kb windows using mosdepth 0.2.9 (Pedersen &
280 Quinlan, 2018). For a given sample, normalized coverage for each window was calculated by
281 dividing the coverage value by the median of all values in R (v. 4.2.1) (R Core Team, 2022).
282 SNPs and short indels were detected using Freebayes 1.3.1 (Garrison & Marth, 2012), with a
283 filter on the minimum fraction of observations supporting a variant (F = 0.03), disabling
284 population priors (-k argument) and using an aggregate probability of observation balance
285 between alleles (-a argument). Variants were then filtered using a custom R script. This script

286 selected only variable positions for which the read total depth was over 200 and for which the
287 alternative allele was supported by at least 10 reads within a tissue (*Wolbachia* genome
288 coverage - mean ± se: ovaries = 723.9 reads ± 134.8, nerve chain = 769.8 ± 81.0, haemolymph
289 = 533.7).

290 ## 2.7 Variant validation

291 As the *A. vulgare* lineage used in our experiments may contain nuclear inserts absent from the
292 reference genome used for read mapping (Chebbi et al., 2019) the risk that sequences from
293 *Wolbachia*-derived nuclear inserts generated spurious SNPs may not have been eliminated.
294 To exclude remaining spurious SNPs, we implemented a three-step approach. (**1**) We checked
295 that the sequences containing candidate SNPs were absent from uninfected individuals
296 sequenced in previous studies, using all short-read data generated by (Chebbi et al., 2019) and
297 (Cordaux et al., 2021). These data constitute whole genome sequences of six pools of 10 males
298 or females and five individuals, from three uninfected lineages. We aligned these short reads
299 with bwa-mem2 on the *w*VulC reference sequence. On the 11 resulting alignment files, variant
300 calling was carried out with the same parameters as above, but only at positions of detected
301 candidate *Wolbachia* variants. All variants for which the alternative allele was present in the
302 reads sequenced from uninfected individuals were eliminated. We then defined a 300-bp
303 window around the position of each remaining variant (starting 150 bp before the site) and
304 excluded variants in windows containing at least two reads from uninfected individuals. (**2**) To
305 further check that each remaining variable region was absent from uninfected individuals, we
306 then designed PCR primers to amplify 120-250 bp targets encompassing the focal variant.
307 These primers were tested on two females from the recipient lineage (i.e., uninfected by
308 *Wolbachia*), on two females from the source line (i.e., infected by *Wolbachia*) and on two of
309 their brothers (not infected by *Wolbachia,* since infection induces feminization). If the primers

310 amplified DNA from at least one non-infected host, then the variant was eliminated. (**3**)
311 Finally, we checked whether sequencing reads carrying non-reference SNP alleles represented
312 sequences that were exceedingly divergent from the reference strain (e.g., insertions of
313 *Wolbachia* DNA into the host genome, or a related bacterium). To do so, we automatically
314 analyzed every candidate SNP via a script that parses the alignment (.bam) files of reads
315 generated in this experiment. This script records the proportion of clipped reads, the
316 proportion of read pairs that were aligned in proper pairs and the number of mismatches
317 between reads and the reference (excluding the SNP itself). The script then performs Fisher
318 exact tests to evaluate if these proportions significantly differ between reads carrying the
319 reference allele and reads carrying the alternativeallele. Any SNP for which the p-value of any
320 test was below 5% (after false discovery rate correction) was excluded. Lastly, the sequencing
321 depth around SNPs that had passed all filters was averaged over 100-bp windows, via samtools
322 depth, and plotted to check for anomalies, mainly the presence of collapsed repeated regions
323 not fully resolved in the *Wolbachia* reference genome assembly.

324 To predict the effect of retained SNPs and indels on proteins coded by annotated
325 genes, we used SNPeff 5.2c (Cingolani et al., 2012). Functional domains in these proteins were
326 annotated using the InterProScan online service (http://www.ebi.ac.uk/interpro/, database
327 release 100.0, (Paysan-Lafosse et al., 2023)).

328 2.8 Screening for variants in maternal lines

329 To determine whether the *Wolbachia* variant(s) validated by our filtration procedure (see
330 above) arose during the focal individuals' lifetime or were maternally inherited, we searched
331 for these variants in their maternal lineage. Specifically, we extracted DNA from the ovaries of
332 sisters and maternal ancestors of focal individuals, going back six generations thanks to our
333 broodstock collection stored at -20°C. The variants as well as the *Wolbachia* reference lineage

334 were searched by amplification-refractory mutation system (ARMS, (C. R. Newton et al.,
335 1989)). For this purpose, for each variant we designed a couple of primers targeting either the
336 reference allele or the variant allele (see primers in appendix 1). ARMS analyses were
337 performed in a 25 µl reaction volume containing 0.5 µl genomic DNA, 5 µl 5X buffer (Promega),
338 0.5 µl dNTP, 1.25 µl forward and reverse primers and 0.125 µl GoTaq® polymerase (Promega).
339 The volume was adjusted to 25 µl with double-distilled water. PCR regimen was as follows:
340 initial denaturation at 95°C for 5 min, followed by 35 cycles for 30 s at 95°C, 30 s at 61°C, 30 s
341 at 72°C, and then a final extension for 5 min at 72°C, and finally the PCR products were
342 maintained at 4°C in the end. PCR products were separated on a 1.5% agarose gel (23min.,
343 100V).

344 ## 2.9 Statistical Analyses

345 Statistical analyses were carried out using the R software (R Core Team, 2022). The influence
346 of the tissular origin of the injected *Wolbachia* on *A. vulgare* mortality was evaluated using
347 the 'survreg' function with either exponential or Weibull errors distribution ('survival'
348 package, (Therneau et al., 2024)). The model included survival as a response variable, and
349 infection status (i.e., injected with *Wolbachia*-infected or uninfected tissue filtrate), tissue
350 origin of the injected filtrate and experimental block as explanatory variables. The influence
351 of *Wolbachia* tissue origin on its ability to colonize and infect different focal tissues of recipient
352 hosts over time was assessed using a generalized linear mixed model (GLMM). Log-
353 transformed relative quantification (RQ) values representing the per-host cell *Wolbachia* dose
354 were fitted as a response variable, assuming normal error distribution. The tissular origin of
355 *Wolbachia*, the focal tissue of recipient injected hosts and the day post injection were used as
356 explanatory variables. The quadratic term day post injection was added to assess whether it
357 significantly improved the model fit. Individual IDs nested in experimental block were

358 specified as random-effect variables in the model. To compare *Wolbachia* loads measured in
359 the tissues of recipient hosts six months after experimental infection with that measured in
360 the same tissues from females of the same age but naturally infected by *Wolbachia* (from the
361 WXw line), we ran, for each tissue, a linear model with log-transformed relative quantification
362 (RQ) values fitted as a response variable and the origin of the individuals (i.e., naturally
363 infected or experimentally infected) as an explanatory variable.

364 Maximal models including all higher-order interactions were simplified by sequentially
365 eliminating non-significant terms and interactions to establish a minimal model (Crawley,
366 2012). The significance of the effects of explanatory variables was established using a
367 likelihood ratio test (LRT, (Crawley, 2012)) whose statistics approximately follows a Chi-square
368 distribution (Bolker, 2008) or an F test. The significant LRT or F value given in the Results
369 section are for the minimal model, whereas non-significant values correspond to those
370 obtained before the deletion of the variables from the model. *A posteriori* contrasts were
371 carried out by aggregating factor levels together and by testing the fit of the simplified model
372 using a likelihood-ratio test (Bolker, 2008; Crawley, 2012).

373 3. Results

374 3.1 *Wolbachia* infection does not significantly influence host survival

375 Under the assumption of both exponential errors and non-constant hazard, no effect of
376 *Wolbachia* tissue origin on the survival rate of *A. vulgare* during early stage of infection (from
377 day 0 to 60, trans-infection experiment 1) was detected (exponential errors: LRT = 0.600, p =
378 0.740, Weibull errors: LRT = 0.602, p = 0.741, **Fig. 1A**). Overall, the injection of *Wolbachia*,
379 irrespective of its tissue origin, was not shown to influence the survival of individuals
380 (exponential errors: LRT = 1.040, p = 0.308, Weibull errors: LRT = 1.039, p = 0.307). Sixty days

381 after injection, the survival rate of infected individuals was 0.87 (± 95% CI, ± 0.79-0.96),
382 compared to 0.80 (± 0.71-0.91) for control animals.

383 In the trans-infection batches used to investigate the influence of *Wolbachia* tissue
384 origin on its ability to persist in recipient host tissue (trans-infection experiment 2), the
385 mortality of animals was also not significantly influenced by *Wolbachia* tissue origin
386 (exponential errors: LRT = 2.65, p = 0.265, Weibull errors: LRT = 2.88, p = 0.236) or even just
387 by the fact of being infected by the bacteria (whatever the origin of the tissue, exponential
388 errors: LRT = 2.22, p = 0.136, Weibull errors: LRT = 2.45, p = 0.117, **Fig. 1B**). The survival rate
389 of infected individuals 200 days after the experimental infection was 0.59 ± 0.48-0.74 and 0.47
390 ± 0.36-0.61 for infected and control animals respectively.

391 3.2 The tissue origin of *Wolbachia* influences its early infection dynamics in recipient
392 host tissues (trans-infection experiment 1)

393 After injection, the presence of *Wolbachia* was detected by qPCR in the three tested tissues
394 of all recipient hosts, confirming its ability to colonize a new host. *Wolbachia* density increased
395 over time (post-injection day: LRT = 16.239, p < 0.0001) and fitting the quadratic term
396 (day_post_injection^2) strongly improved model fit (LRT = 32.181, p < 0.0001), suggesting that
397 *Wolbachia* burden was more accurately modelled by an accelerated polynomial function of
398 day post-injection (**Fig. 2A**). The density of *Wolbachia* in tissues started very low on day 20
399 post-injection, then rose slightly between day 20 and day 40, to drastically increase between
400 day 40 and day 60 post-injection. Although the pattern of infection in the different recipient
401 tissues was overall similar, *Wolbachia* load was significantly influenced by the interaction
402 between the colonized recipient tissue and the day post-injection (LRT = 74.309, p < 0.0001).
403 The dynamics of infection within the nerve chain were significantly different from those

404 observed in the haemolymph and ovaries, leading to a higher bacterial load in nerve tissues
405 60 days post-infection (LRT = 57.228, $p < 0.0001$, LRT = 122.240, $p < 0.0001$, respectively, **Fig.**
406 **2A**). The dynamics of infection were also significantly different within haemolymph and
407 ovaries (LRT = 17.771, $p = 0.0013$, **Fig. 2A**), as bacterial load was lower in ovaries at the end of
408 monitoring (mean RQ ± se, nerve chain = 6.582 ± 1.596, haemolymph = 4.864 ± 1.612, ovaries
409 = 2.533 ± 0.594, **Fig. 2A**). *Wolbachia* infection dynamics were also influenced by the tissue
410 origin of the injected bacteria (interaction between days post-injection and tissue origin: LRT
411 = 24.205, $p < 0.0001$). Whether the bacteria came from the haemolymph or ovaries of
412 naturally infected animals did not significantly affect the colonization dynamics of *Wolbachia*
413 in the injected recipients (LRT = 0.647, $p = 0.723$, **Fig. 2B**). However, bacteria from the nerve
414 chain colonized recipient hosts less rapidly than bacteria from other tissues (nerve chain
415 versus haemolymph: LRT = 28.981, $p < 0.0001$, nerve chain versus ovaries: LRT = 33.64, $p <$
416 0.0001). At 60 days post-injection, the *Wolbachia* load was on average more than twice as
417 high when the bacteria came from the ovaries and haemolymph than when they came from
418 the nerve chain of infected source hosts (mean RQ ± se, ovaries = 8.191 ± 2.18, haemolymph
419 = 5.26 ± 1.077, nerve chain = 0.899 ± 0.197, **Fig. 2B**). However, there was no significant
420 interaction between the colonized recipient tissue and the *Wolbachia's* original tissue,
421 suggesting that bacteria originating from a tissue do not colonize that same tissue more
422 effectively in recipient hosts (LRT = 6.957, $p = 0.138$).

423 ### 3.3 The tissue origin of *Wolbachia* does not influence significantly its persistence in
424 recipient host tissues (trans-infection experiment 2)

425 *Wolbachia* densities at 200 days after infection were significantly different between tissues
426 from the recipient hosts (LRT = 39.224, $p < 0.0001$, **Fig. 3**). Bacterial load was the highest in

427 the nerve chain and the lowest in the haemolymph (contrast analyses, haemolymph versus
428 nerve chain: LRT = 38.133, $p < 0.0001$, haemolymph versus ovaries: LRT = 20.823, $p < 0.0001$,
429 nerve chain versus ovaries: LRT = 6.969, $p = 0.008$, **Fig. 3**). The bacterial load in the ovaries and
430 haemolymph of recipient females were similar to those observed in the same tissues of
431 females naturally infected by *Wolbachia* (source lineage, F = 0.184, $p = 0.672$, F = 0.268, $p =$
432 0.609, respectively, **Fig. 3 & 4**). In contrast, bacterial density in the nerve chain of
433 experimentally infected females was on average more than twice that measured in the nerve
434 chain of naturally infected individuals (F = 38.089, $p < 0.0001$, **Fig. 3 & 4**).

435 Contrary to what was observed during the early phase of infection, there was no effect
436 of the tissue origin of *Wolbachia* on the bacterial load in recipient tissues at 200 days post-
437 injection (LRT = 0.368, $p = 0.832$). Similarly, *Wolbachia* density in recipient tissues was not
438 influenced by the interaction between the colonized tissue and the tissue origin of the injected
439 bacteria (LRT = 9.539, $p = 0.059$).

440 3.4 Complete genome assembly of the *w*VulC *Wolbachia* strain

441 Using ONT reads, a complete circular genome sequence (1,638,144 bp) of the *w*VulC
442 *Wolbachia* strain was assembled. The estimated completeness of the assembly was very high,
443 with 99.8% of the expected BUSCO genes found in the sequence (C: 99.8% [S: 99.5%, D: 0.3%],
444 F: 0.0%). The annotation of the genome resulted in 1,390 protein-coding sequences and 208
445 pseudogenes (**Fig. 5**). The *w*VulC genome contained 138 IS elements that are larger than 150
446 bp, representing 8.45% of the total length of the genome. This high proportion of repeated
447 sequences for a bacterium is similar to that of other *Wolbachia* strains (Cerveau et al., 2011).
448 We also identified seven prophage regions (six intact and one questionable region, following
449 PHASTEST scoring criteria), representing 12.1% of the *w*VulC genome.

450 ### 3.5 Whole-genome resequencing and variant calling reveal *Wolbachia* genome stability

451 The variant calling performed using the whole-genome resequencing of tissues from three
452 females naturally infected by *Wolbachia* (i.e., source lineage) detected 641 SNPs and short
453 indels. However, 584 of these apparent variants were also detected in the resequenced
454 genome of several *A. vulgare* lineages not infected by *Wolbachia* (validation procedure, step
455 1), meaning that these variants probably amounted to *Wolbachia* sequences inserted into the
456 host nuclear genome. The presence of reads sequenced from uninfected hosts within a 300-
457 bp window around the 57 remaining polymorphic regions resulted in the exclusion of 26
458 variants (validation procedure step 2). Of the remaining 31 SNPs and small indels, 7 were
459 excluded because their regions were PCR-amplified in males not infected with *Wolbachia*
460 (infection status confirmed by qPCR, validation procedure step 3). Finally, in the last step of
461 variant validation, we excluded 23 variants due to anomalies detected, such as a high
462 proportion of clipped reads and/or a high number of mismatches between reads and
463 reference. Overall, only 0.15% (one SNP) of the originally detected variants were finally
464 validated. This unique SNP was observed in a single individual (F_1999). The frequency of this
465 variant varied slightly among the three tissues (**Table 1**). The mutation affected a protein-
466 coding gene, with a non-synonymous substitution (**Table 1**, **Fig. 5**). The putative protein did
467 not have any recognized functional domain. The variant was not detected in the F_1999
468 individual's sisters, and was also absent from all females tested in the maternal line (traced
469 back 6 generations, see appendix 1).

470 ## 4. Discussion

471 Experimental trans-infections enabled us to study the influence of the tissue origin of
472 *Wolbachia* on the early infection dynamics of the endosymbiont in different recipient host

473 tissues, and the ability of each bacterial sub-population to establish a chronic infection. At the
474 same time, regular monitoring of injected individuals over a period of six months shed light
475 on the influence of *Wolbachia* on the survival rate of recipient hosts and did not reveal any
476 difference between *Wolbachia* sub-populations with respect to their virulence. In addition,
477 our results corroborate a previous report showing a similar survival rate between trans-
478 infected and un-infected animals (Le Clec'h et al., 2012). As the source and recipient lines
479 belonged to the same field-collected *A. vulgare* population, they should be ecologically similar
480 for *Wolbachia*. Low virulence is therefore expected, as for most vertically transmitted
481 endosymbionts transferred between closely related hosts (Le Clec'h et al., 2013).

482 Colonization of recipient female tissues was relatively fast, with a threefold increase in
483 *Wolbachia* density between the second and sixth month after infection. At the end of the
484 experiment, the bacterial load in the tissues of the recipient females was similar to, or even
485 higher than, that observed in the tissues of naturally vertically infected females.

486 Nevertheless, although rapid, the dynamics of *Wolbachia* infection varied according to
487 the tissue origin of the bacteria. Bacteria from the nerve chain colonized recipient hosts much
488 less rapidly than bacteria from ovaries and haemolymph. Two months after infection with a
489 similar dose of bacteria, *Wolbachia* load was more than twice as low in hosts injected with
490 bacteria from nerve chain, compared with hosts infected by bacteria from the other two
491 tissues. The growth rate of bacteria is known to largely vary according to the type and amount
492 of nutrients available in their environment (Keiblinger et al., 2010; Liu et al., 2005). The lower
493 growth rate of bacteria from nerve chain, compared with those from the other tissues, could
494 therefore be explained by the fact that in naturally infected hosts, this tissue is less favourable
495 to the development of *Wolbachia* (e.g., poorer in resources). If so, bacteria from the nerve
496 chain could be subject to growth-limiting stress at the time of their horizontal transfer, which

497 would explain their lower replication rate within the recipient host at the start of infection.
498 However, the nerve chain was the recipient host tissue the most rapidly colonized by
499 *Wolbachia* after trans-infection, and the one showing the highest bacterial load at each
500 sampling point irrespective of the tissue origin of the bacteria. As well as showing no tropism
501 towards the tissue of origin, this result suggests that nervous tissue is actually favourable to
502 the development of *Wolbachia.*

503 Alternatively, the lower growth rate from bacteria originating from the nerve chain
504 could be adaptive. Classic theory for the evolution of virulence is based on a trade-off between
505 parasite growth, transmission and host survival, which predicts that higher growth increases
506 not only transmission but also virulence (Alizon et al., 2009; Frank, 1996). *Wolbachia*
507 transmission is essentially maternal (Turelli et al., 2018; Werren et al., 2008), but cases of non-
508 maternal transmission have been observed *in natura* (Durand et al., 2024; Sanaei et al., 2021)
509 and in the laboratory (Le Clec'h et al., 2013; Rigaud & Juchault, 1995). In a tissue not directly
510 involved in parasite transmission, we predicted that virulence should constrain the parasite
511 growth to low levels. Our results corroborate this prediction, as *Wolbachia* from the nerve
512 chain of *A. vulgare* should not be transmissible – except maybe in rare cases of cannibalism
513 and predation (Le Clec'h et al., 2013) – and may prove detrimental to the host if they
514 proliferate. Uncontrolled colonization of nerve cells has indeed been shown to alter host
515 behaviour in several *Wolbachia*-host pairs (Bi & Wang, 2020; Le Clec'h et al., 2012), and to
516 lead to severe tissue degeneration and premature host death (Kosmidis et al., 2014; W. L. Le
517 Clec'h et al., 2012; Min & Benzer, 1997; Strunov & Kiseleva, 2016). In tissues that allow
518 parasite transmission, the balance between *Wolbachia* growth and host fitness should favour
519 higher growth rates. In terrestrial isopods, both ovaries and haemolymph play a key role in
520 both intra- and inter-host dissemination of *Wolbachia*. Ovaries are the route for vertical

521 transmission and haemolymph, in addition to participating in the dissemination of the bacteria
522 across host tissues (Braquart-Varnier et al., 2015; Sanaei et al., 2021), may also be involved in
523 horizontal transfer via contact between injured individuals (Rigaud & Juchault, 1995).

524 Although initial differences were observed at two months post-infection, the tissue
525 origin of the injected *Wolbachia* had no significant effect on bacterial load in the three tissues
526 analysed four months later (i.e., 6 months post-injection). The convergence of growth rates
527 over time suggests that the early phenotypic variability observed two months post-infection
528 may result from phenotypic plasticity. This interpretation is further supported by the absence
529 of recurrent small genomic variations associated with tissue types in naturally infected
530 individuals from the source lineage. More broadly, SNP and small indel analyses revealed a
531 single substitution detected across sequence data from seven tissue samples. This SNP,
532 observed in one female (F_1999), was nevertheless present in all three *Wolbachia*
533 subpopulations, with allelic frequencies ranging from 24% to 58% depending on the tissue.
534 This mutation, located in a gene coding for a protein of unknown function, leads to an amino
535 acid substitution. Although we currently have no information on the phenotypic impact of this
536 mutation, amino acid substitution may have strong phenotypic effects in bacteria (e.g.,
537 (Abdelaal et al., 2009; Bacigalupe et al., 2019)).

538 The variant, although predominant in the nerve chain, was present at lower
539 frequencies in the ovaries. Nevertheless, over a quarter of the *Wolbachia* population in this
540 tissue carried the mutation. This suggests that some of the female's oocytes may have been
541 colonized by the variant and that, despite the suspicion of a strong bottleneck, it could have
542 passed it on to its offspring (Chrostek & Teixeira, 2015). However, this hypothesis could not
543 be verified in our study, as the female was sacrificed before reproducing. What is clear is that
544 the absence of this SNP within the individual's maternal lineage strongly suggests that this

545 *Wolbachia* variant arose during its lifetime. The emergence of *Wolbachia* variants within just
546 a few host generations or even during a host's lifetime has been documented (Chrostek &
547 Teixeira, 2018; Martinez & Sinkins, 2023; Namias et al., 2024; Newton & Sheehan, 2015).
548 However, most reported variants were associated with structural genomic changes rather
549 than point genomic mutations (e.g., (Chrostek & Teixeira, 2018; Namias et al., 2024)). We
550 currently have no information on the presence of structural genomic changes within the
551 different *Wolbachia* tissular subpopulations, but in agreement with reports from other
552 symbiotic systems, the very low number of point mutations observed in our study tends to
553 support the stability of the *Wolbachia* genome (Dainty et al., 2021; Huang et al., 2020; Ross et
554 al., 2022; Trouche et al., 2024).

555 In conclusion, our study reveals that within-host environmental heterogeneity can lead
556 to diverse phenotypes in the most widespread bacterial endosymbiont in animals, *Wolbachia*.
557 This variability did not appear to result from genomic variation, but from phenotypic plasticity.
558 From a methodological point of view, we showed that the detection of variants in
559 endosymbiont populations requires considerable caution, as our conservative approach led
560 us to exclude more than 99.85% of the initially called variants. We recommend the use of a
561 rigorous step-by-step approach to eliminate spurious genetic variants caused by the presence
562 of endosymbiont genomic sequences inserted into the host genome.

563 **Data accessibility statement**

564 The R scripts and data supporting the conclusions of this article are available on the Figshare
565 data repository (https://figshare.com/s/b1f84643b65b4f897c54). To ensure the stability and
566 reliability of the command-lines used for genome assembly and SNP calling we have included
567 all necessary information and options in the github repository (https://github.com/UMR-
568 CNRS-7267/Wolbachia_endosymbiont_heterogeneity_paper). We have taken proactive

measures to address potential volatility on GitHub by uploading a compressed archive of this GitHub methodology to the Figshare data repository. Raw sequencing data have been deposited in GenBank (*w*VulC genome assembly: BioProject PRJNA1116085; *Wolbachia* resequencing: PRJNA1117639).

Author's contributions

R.P. and R.C. conceived and designed the experiments. R.P., R.J., M.P. and M.R. performed the trans-infection experiments. RP, TU, WA performed the preliminary experiment. RP and C.D prepared the samples for resequencing and C.D, TB and TU carried out the PCRs. D.O. performed *Wolbachia* genome sequencing. Y.D. assembled the *Wolbachia* genome. R.P., Y.D., B.M. and J.P. analysed the data. R.P. wrote the first draft of the manuscript, and all authors contributed substantially to revision.

Competing interests

We declare we have no competing interests.

Funding

This work was funded by Agence Nationale de la Recherche Grants ANR-21-CE02-0004 (RESIST) to RC and ANR-20-CE02-004 (SymChroSex) to JP, and intramural funds from the CNRS and the University of Poitiers.

Acknowledgements

We thank Isabelle Giraud for the extraction of the DNA used to sequence and assemble the genome of *Wolbachia w*VulC and Pierre Grève and Didier Bouchon for providing us with preliminary data so that we could fine-tune the bioinformatics analyses. We would like to thank Alexandra Lafitte for her invaluable work supervising the breeding of *A. vulgare*.

592 ## 5. References

593 Abdelaal, A., El-Ghaffar, H. A., Zaghloul, M. H. E., El Mashad, N., Badran, E., & Fathy, A.
594 (2009). Genotypic detection of rifampicin and isoniazid resistant *Mycobacterium*
595 *tuberculosis* strains by DNA sequencing: A randomized trial. *Annals of Clinical*
596 *Microbiology and Antimicrobials*, *8*(1), 4. https://doi.org/10.1186/1476-0711-8-4
597 Ailloud, F., Didelot, X., Woltemate, S., Pfaffinger, G., Overmann, J., Bader, R. C., Schulz, C.,
598 Malfertheiner, P., & Suerbaum, S. (2019). Within-host evolution of *Helicobacter pylori*
599 shaped by niche-specific adaptation, intragastric migrations and selective sweeps.
600 *Nature Communications*, *10*(1), Article 1. https://doi.org/10.1038/s41467-019-10050-
601 1
602 Alizon, S., Hurford, A., Mideo, N., & Van Baalen, M. (2009). Virulence evolution and the
603 trade-off hypothesis: History, current state of affairs and the future. *Journal of*
604 *Evolutionary Biology*, *22*(2), 245–259. https://doi.org/10.1111/j.1420-
605 9101.2008.01658.x
606 Avettand-Fenoel, V., Hocqueloux, L., Müller-Trutwin, M., Prazuck, T., Melard, A., Chaix, M.-L.,
607 Agoute, E., Michau, C., & Rouzioux, C. (2011). Greater diversity of HIV DNA variants in
608 the rectum compared to variants in the blood in patients without HAART. *Journal of*
609 *Medical Virology*, *83*(9), 1499–1507. https://doi.org/10.1002/jmv.22132
610 Bacigalupe, R., Tormo-Mas, M. Á., Penadés, J. R., & Fitzgerald, J. R. (2019). A multihost
611 bacterial pathogen overcomes continuous population bottlenecks to adapt to new
612 host species. *Science Advances*, *5*(11), eaax0063.
613 https://doi.org/10.1126/sciadv.aax0063

Ben-Hur, E., & Kadmon, R. (2020). Heterogeneity–diversity relationships in sessile organisms: A unified framework. *Ecology Letters*, *23*(1), 193–207. https://doi.org/10.1111/ele.13418

Bessière, P., & Volmer, R. (2021). From one to many: The within-host rise of viral variants. *PLOS Pathogens*, *17*(9), e1009811. https://doi.org/10.1371/journal.ppat.1009811

Bi, J., & Wang, Y. (2020). The effect of the endosymbiont *Wolbachia* on the behavior of insect hosts. *Insect Science*, *27*(5), 846–858. https://doi.org/10.1111/1744-7917.12731

Bolker, B. M. (2008). *Ecological Models and Data in R*. Princeton, Princeton University Press.

Braquart-Varnier, C., Raimond, M., Mappa, G., Chevalier, F. D., Le Clec'h, W., & Sicard, M. (2015). The Hematopoietic organ: A cornerstone for *Wolbachia* propagation between and within Hosts. *Frontiers in Microbiology*, *6*. https://doi.org/10.3389/fmicb.2015.01424

Burnett, M. R., August, P. V., Brown, J. H., & Killingbeck, K. T. (1998). The influence of geomorphological heterogeneity on biodiversity: I. A patch-scale perspective. *Conservation Biology*, *12*(2), 363–370.

Cerveau, N., Leclercq, S., Leroy, E., Bouchon, D., & Cordaux, R. (2011). Short- and Long-term evolutionary dynamics of bacterial insertion sequences: Insights from *Wolbachia* endosymbionts. *Genome Biology and Evolution*, *3*, 1175–1186. https://doi.org/10.1093/gbe/evr096

Chebbi, M. A., Becking, T., Moumen, B., Giraud, I., Gilbert, C., Peccoud, J., & Cordaux, R. (2019). The Genome of *Armadillidium vulgare* (Crustacea, Isopoda) provides insights into sex chromosome evolution in the context of cytoplasmic sex determination.

Molecular Biology and Evolution, *36*(4), 727–741. https://doi.org/10.1093/molbev/msz010

Chen, S., Zhou, Y., Chen, Y., & Gu, J. (2018). fastp: An ultra-fast all-in-one FASTQ preprocessor. *Bioinformatics*, *34*(17), i884–i890. https://doi.org/10.1093/bioinformatics/bty560

Chrostek, E., & Teixeira, L. (2015). Mutualism breakdown by amplification of *Wolbachia* genes. *PLOS Biology*, *13*(2), e1002065. https://doi.org/10.1371/journal.pbio.1002065

Chrostek, E., & Teixeira, L. (2018). Within host selection for faster replicating bacterial symbionts. *PLoS ONE*, *13*(1). https://doi.org/10.1371/journal.pone.0191530

Cingolani, P., Platts, A., Wang, L. L., Coon, M., Nguyen, T., Wang, L., Land, S. J., Lu, X., & Ruden, D. M. (2012). A program for annotating and predicting the effects of single nucleotide polymorphisms, SnpEff: SNPs in the genome of *Drosophila melanogaster* strain w1118; iso-2; iso-3. *Fly*, *6*(2), 80–92. https://doi.org/10.4161/fly.19695

Clement, S., Vaudaux, P., Francois, P., Schrenzel, J., Huggler, E., Kampf, S., Chaponnier, C., Lew, D., & Lacroix, J.-S. (2005). Evidence of an intracellular reservoir in the nasal mucosa of patients with recurrent *Staphylococcus aureus* rhinosinusitis. *The Journal of Infectious Diseases*, *192*(6), 1023–1028. https://doi.org/10.1086/432735

Cordaux, R., Chebbi, M. A., Giraud, I., Pleydell, D. R. J., & Peccoud, J. (2021). Characterization of a sex-determining region and its genomic context via statistical estimates of haplotype frequencies in daughters and sons sequenced in pools. *Genome Biology and Evolution*, *13*(8), evab121. https://doi.org/10.1093/gbe/evab121

Cordaux, R., & Gilbert, C. (2017). Evolutionary significance of *Wolbachia*-to-animal horizontal gene transfer: Female sex determination and the f element in the isopod *Armadillidium vulgare*. *Genes*, *8*(7), 186. https://doi.org/10.3390/genes8070186

661 Cordaux, R., Michel-Salzat, A., Frelon-Raimond, M., Rigaud, T., & Bouchon, D. (2004).
662 Evidence for a new feminizing *Wolbachia* strain in the isopod *Armadillidium vulgare*:
663 evolutionary implications. *Heredity*, *93*(1), 78–84.
664 https://doi.org/10.1038/sj.hdy.6800482
665 Crawley, M. J. (2012). *The R Book*. John Wiley & Sons.
666 Dainty, K. R., Hawkey, J., Judd, L. M., Pacidônio, E. C., Duyvestyn, J. M., Gonçalves, D. S., Lin,
667 S. Y., O'Donnell, T. B., O'Neill, S. L., Simmons, C. P., Holt, K. E., & Flores, H. A. (2021).
668 wMel *Wolbachia* genome remains stable after 7 years in Australian *Aedes aegypti*
669 field populations. *Microbial Genomics*, *7*(9), 000641.
670 https://doi.org/10.1099/mgen.0.000641
671 Danecek, P., Bonfield, J. K., Liddle, J., Marshall, J., Ohan, V., Pollard, M. O., Whitwham, A.,
672 Keane, T., McCarthy, S. A., Davies, R. M., & Li, H. (2021). Twelve years of SAMtools
673 and BCFtools. *GigaScience*, *10*(2), giab008.
674 https://doi.org/10.1093/gigascience/giab008
675 De Coster, W., D'Hert, S., Schultz, D. T., Cruts, M., & Van Broeckhoven, C. (2018). NanoPack:
676 Visualizing and processing long-read sequencing data. *Bioinformatics (Oxford,*
677 *England)*, *34*(15), 2666–2669. https://doi.org/10.1093/bioinformatics/bty149
678 Depeux, C., Branger, A., Paulhac, H., Pigeault, R., & Beltran-Bech, S. (2024). Deleterious
679 effects of *Wolbachia* on life history and physiological traits of common pill woodlice.
680 *Journal of Invertebrate Pathology*, *207*, 108187.
681 https://doi.org/10.1016/j.jip.2024.108187
682 Didelot, X., Walker, A. S., Peto, T. E., Crook, D. W., & Wilson, D. J. (2016). Within-host
683 evolution of bacterial pathogens. *Nature Reviews. Microbiology*, *14*(3), 150–162.
684 https://doi.org/10.1038/nrmicro.2015.13

Durand, S., Lheraud, B., Giraud, I., Bech, N., Grandjean, F., Rigaud, T., Peccoud, J., & Cordaux, R. (2023). Heterogeneous distribution of sex ratio distorters in natural populations of the isopod *Armadillidium vulgare*. *Biology Letters*, *19*(1), 20220457. https://doi.org/10.1098/rsbl.2022.0457

Durand, S., Pigeault, R., Giraud, I., Loisier, A., Bech, N., Grandjean, F., Rigaud, T., Peccoud, J., & Cordaux, R. (2024). Temporal stability of sex ratio distorter prevalence in natural populations of the isopod *Armadillidium vulgare*. *Heredity*, 1–11. https://doi.org/10.1038/s41437-024-00713-1

Frank, S. A. (1996). Models of parasite virulence. *The Quarterly Review of Biology*, *71*(1), 37–78. https://doi.org/10.1086/419267

Garrison, E., & Marth, G. (2012). *Haplotype-based variant detection from short-read sequencing* (No. arXiv:1207.3907). arXiv. https://doi.org/10.48550/arXiv.1207.3907

Gupta, K., Toelzer, C., Williamson, M. K., Shoemark, D. K., Oliveira, A. S. F., Matthews, D. A., Almuqrin, A., Staufer, O., Yadav, S. K. N., Borucu, U., Garzoni, F., Fitzgerald, D., Spatz, J., Mulholland, A. J., Davidson, A. D., Schaffitzel, C., & Berger, I. (2022). Structural insights in cell-type specific evolution of intra-host diversity by SARS-CoV-2. *Nature Communications*, *13*(1), Article 1. https://doi.org/10.1038/s41467-021-27881-6

Haft, D. H., Badretdin, A., Coulouris, G., DiCuccio, M., Durkin, A. S., Jovenitti, E., Li, W., Mersha, M., O'Neill, K. R., Virothaisakun, J., & Thibaud-Nissen, F. (2024). RefSeq and the prokaryotic genome annotation pipeline in the age of metagenomes. *Nucleic Acids Research*, *52*(D1), D762–D769. https://doi.org/10.1093/nar/gkad988

Houle, C., Pelletier, F., Bélisle, M., & Garant, D. (2020). Impacts of environmental heterogeneity on natural selection in a wild bird population. *Evolution*, *74*(6), 1142–1154. https://doi.org/10.1111/evo.13939

Huang, B., Yang, Q., Hoffmann, A. A., Ritchie, S. A., Hurk, A. F. van den, & Warrilow, D. (2020). *Wolbachia* genome stability and mtDNA variants in *Aedes aegypti* field populations eight years after release. *iScience*, *23*(10). https://doi.org/10.1016/j.isci.2020.101572

Huang, B.-H., Huang, C.-W., Huang, C.-L., & Liao, P.-C. (2017). Continuation of the genetic divergence of ecological speciation by spatial environmental heterogeneity in island endemic plants. *Scientific Reports*, *7*(1), 5465. https://doi.org/10.1038/s41598-017-05900-1

Huang, Y., Tran, I., & Agrawal, A. F. (2016). Does genetic variation maintained by environmental heterogeneity facilitate adaptation to novel selection? *The American Naturalist*, *188*(1), 27–37. https://doi.org/10.1086/686889

Hunt, M., Silva, N. D., Otto, T. D., Parkhill, J., Keane, J. A., & Harris, S. R. (2015). Circlator: automated circularization of genome assemblies using long sequencing reads. *Genome Biology*, *16*(1), 294. https://doi.org/10.1186/s13059-015-0849-0

Ioannidis, P., Hotopp, J. C. D., Sapountzis, P., Siozios, S., Tsiamis, G., Bordenstein, S. R., Baldo, L., Werren, J. H., & Bourtzis, K. (2007). New criteria for selecting the origin of DNA replication in *Wolbachia* and closely related bacteria. *BMC Genomics*, *8*(1), 182. https://doi.org/10.1186/1471-2164-8-182

Johnson, P. T. J., Wood, C. L., Joseph, M. B., Preston, D. L., Haas, S. E., & Springer, Y. P. (2016). Habitat heterogeneity drives the host-diversity-begets-parasite-diversity relationship: Evidence from experimental and field studies. *Ecology Letters*, *19*(7), 752–761. https://doi.org/10.1111/ele.12609

Jorth, P., Staudinger, B. J., Wu, X., Hisert, K. B., Hayden, H., Garudathri, J., Harding, C. L., Radey, M. C., Rezayat, A., Bautista, G., Berrington, W. R., Goddard, A. F., Zheng, C.,

Angermeyer, A., Brittnacher, M. J., Kitzman, J., Shendure, J., Fligner, C. L., Mittler, J., … Singh, P. K. (2015). Regional isolation drives bacterial diversification within cystic fibrosis lungs. *Cell Host & Microbe*, *18*(3), 307–319. https://doi.org/10.1016/j.chom.2015.07.006

Jridi, C., Martin, J.-F., Marie-Jeanne, V., Labonne, G., & Blanc, S. (2006). Distinct Viral Populations differentiate and evolve independently in a single perennial host plant. *Journal of Virology*, *80*(5), 2349–2357. https://doi.org/10.1128/jvi.80.5.2349-2357.2006

Kamiya, T., O'Dwyer, K., Nakagawa, S., & Poulin, R. (2014). Host diversity drives parasite diversity: Meta-analytical insights into patterns and causal mechanisms. *Ecography*, *37*(7), 689–697.

Kaur, R., Shropshire, J. D., Cross, K. L., Leigh, B., Mansueto, A. J., Stewart, V., Bordenstein, S. R., & Bordenstein, S. R. (2021). Living in the endosymbiotic world of *Wolbachia*: A centennial review. *Cell Host & Microbe*, *29*(6), 879–893. https://doi.org/10.1016/j.chom.2021.03.006

Keiblinger, K. M., Hall, E. K., Wanek, W., Szukics, U., Hämmerle, I., Ellersdorfer, G., Böck, S., Strauss, J., Sterflinger, K., Richter, A., & Zechmeister-Boltenstern, S. (2010). The effect of resource quantity and resource stoichiometry on microbial carbon-use-efficiency. *FEMS Microbiology Ecology*, *73*(3), 430–440. https://doi.org/10.1111/j.1574-6941.2010.00912.x

Kolmogorov, M., Yuan, J., Lin, Y., & Pevzner, P. A. (2019). Assembly of long, error-prone reads using repeat graphs. *Nature Biotechnology*, *37*(5), 540–546. https://doi.org/10.1038/s41587-019-0072-8

Kosmidis, S., Missirlis, F., Botella, J. A., Schneuwly, S., Rouault, T. A., & Skoulakis, E. M. C. (2014). Behavioral decline and premature lethality upon pan-neuronal ferritin overexpression in *Drosophila* infected with a virulent form of *Wolbachia*. *Frontiers in Pharmacology*, *5*, 66. https://doi.org/10.3389/fphar.2014.00066

Krzywinski, M., Schein, J., Birol, I., Connors, J., Gascoyne, R., Horsman, D., Jones, S. J., & Marra, M. A. (2009). Circos: An information aesthetic for comparative genomics. *Genome Research*, *19*(9), 1639–1645. https://doi.org/10.1101/gr.092759.109

Langenheder, S., & Lindström, E. S. (2019). Factors influencing aquatic and terrestrial bacterial community assembly. *Environmental Microbiology Reports*, *11*(3), 306–315. https://doi.org/10.1111/1758-2229.12731

Le Clec'h, W. L., Braquart-Varnier, C., Raimond, M., Ferdy, J.-B., Bouchon, D., & Sicard, M. (2012). High Virulence of *Wolbachia* after host switching: When autophagy hurts. *PLOS Pathogens*, *8*(8), e1002844. https://doi.org/10.1371/journal.ppat.1002844

Le Clec'h, W. L., Chevalier, F. D., Genty, L., Bertaux, J., Bouchon, D., & Sicard, M. (2013). Cannibalism and predation as paths for horizontal passage of *Wolbachia* between terrestrial isopods. *PLOS ONE*, *8*(4), e60232. https://doi.org/10.1371/journal.pone.0060232

Le Clec'h, W., Raimond, M., Guillot, S., Bouchon, D., & Sicard, M. (2013). Horizontal transfers of feminizing versus non-feminizing *Wolbachia* strains: From harmless passengers to pathogens. *Environmental Microbiology*, *15*(11), 2922–2936. https://doi.org/10.1111/1462-2920.12172

Leclercq, S., Thézé, J., Chebbi, M. A., Giraud, I., Moumen, B., Ernenwein, L., Grève, P., Gilbert, C., & Cordaux, R. (2016). Birth of a W sex chromosome by horizontal transfer of

Wolbachia bacterial symbiont genome. *Proceedings of the National Academy of Sciences*, *113*(52), 15036–15041. https://doi.org/10.1073/pnas.1608979113

LePage, D., & Bordenstein, S. R. (2013). *Wolbachia*: Can we save lives with a great pandemic? *Trends in Parasitology*, *29*(8), 385–393. https://doi.org/10.1016/j.pt.2013.06.003

Li, W., O'Neill, K. R., Haft, D. H., DiCuccio, M., Chetvernin, V., Badretdin, A., Coulouris, G., Chitsaz, F., Derbyshire, M. K., Durkin, A. S., Gonzales, N. R., Gwadz, M., Lanczycki, C. J., Song, J. S., Thanki, N., Wang, J., Yamashita, R. A., Yang, M., Zheng, C., … Thibaud-Nissen, F. (2021). RefSeq: Expanding the prokaryotic genome annotation pipeline reach with protein family model curation. *Nucleic Acids Research*, *49*(D1), D1020–D1028. https://doi.org/10.1093/nar/gkaa1105

Lieberman, T. D., Wilson, D., Misra, R., Xiong, L. L., Moodley, P., Cohen, T., & Kishony, R. (2016). Genomic diversity in autopsy samples reveals within-host dissemination of HIV-associated *Mycobacterium tuberculosis*. *Nature Medicine*, *22*(12), Article 12. https://doi.org/10.1038/nm.4205

Liu, M., Durfee, T., Cabrera, J. E., Zhao, K., Jin, D. J., & Blattner, F. R. (2005). Global transcriptional programs reveal a carbon source foraging strategy by *Escherichia coli. The Journal of Biological Chemistry*, *280*(16), 15921–15927. https://doi.org/10.1074/jbc.M414050200

Manni, M., Berkeley, M. R., Seppey, M., & Zdobnov, E. M. (2021). BUSCO: Assessing genomic data quality and beyond. *Current Protocols*, *1*(12), e323. https://doi.org/10.1002/cpz1.323

Marçais, G., Delcher, A. L., Phillippy, A. M., Coston, R., Salzberg, S. L., & Zimin, A. (2018). MUMmer4: A fast and versatile genome alignment system. *PLOS Computational Biology*, *14*(1), e1005944. https://doi.org/10.1371/journal.pcbi.1005944

Martinez, J., & Sinkins, S. P. (2023). *Rapid evolution of* Wolbachia *genomes in mosquito cell culture*. Evolutionary Biology. https://doi.org/10.1101/2023.09.20.558649

Mcdonald, J. F., & Ayala, F. J. (1974). Genetic response to environmental heterogeneity. *Nature*, *250*(5467), 572–574. https://doi.org/10.1038/250572a0

Min, K. T., & Benzer, S. (1997). *Wolbachia*, normally a symbiont of *Drosophila*, can be virulent, causing degeneration and early death. *Proceedings of the National Academy of Sciences of the United States of America*, *94*(20), 10792–10796. https://doi.org/10.1073/pnas.94.20.10792

Namias, A., Ngaku, A., Makoundou, P., Unal, S., Sicard, M., & Weill, M. (2024). Intra-lineage microevolution of *Wolbachia* leads to the emergence of new cytoplasmic incompatibility patterns. *PLOS Biology*, *22*(2), e3002493. https://doi.org/10.1371/journal.pbio.3002493

Newton, C. R., Graham, A., Heptinstall, L. E., Powell, S. J., Summers, C., Kalsheker, N., Smith, J. C., & Markham, A. F. (1989). Analysis of any point mutation in DNA. The amplification refractory mutation system (ARMS). *Nucleic Acids Research*, *17*(7), 2503–2516. https://doi.org/10.1093/nar/17.7.2503

Newton, I. L. G., & Sheehan, K. B. (2015). Passage of *Wolbachia pipientis* through mutant *Drosophila melanogaster* induces phenotypic and genomic changes. *Applied and Environmental Microbiology*, *81*(3), 1032–1037. https://doi.org/10.1128/AEM.02987-14

Obaldia, N., Meibalan, E., Sa, J. M., Ma, S., Clark, M. A., Mejia, P., Moraes Barros, R. R., Otero, W., Ferreira, M. U., Mitchell, J. R., Milner, D. A., Huttenhower, C., Wirth, D. F., Duraisingh, M. T., Wellems, T. E., & Marti, M. (2018). Bone marrow is a major

826 parasite reservoir in *Plasmodium vivax* infection. *mBio*, *9*(3).
827 https://doi.org/10.1128/mBio.00625-18
828 Paysan-Lafosse, T., Blum, M., Chuguransky, S., Grego, T., Pinto, B. L., Salazar, G. A., Bileschi,
829 M. L., Bork, P., Bridge, A., Colwell, L., Gough, J., Haft, D. H., Letunić, I., Marchler-
830 Bauer, A., Mi, H., Natale, D. A., Orengo, C. A., Pandurangan, A. P., Rivoire, C., …
831 Bateman, A. (2023). InterPro in 2022. *Nucleic Acids Research*, *51*(D1), D418–D427.
832 https://doi.org/10.1093/nar/gkac993
833 Peccoud, J., Chebbi, M. A., Cormier, A., Moumen, B., Gilbert, C., Marcadé, I., Chandler, C., &
834 Cordaux, R. (2017). Untangling heteroplasmy, structure, and evolution of an atypical
835 mitochondrial genome by PacBio sequencing. *Genetics*, *207*(1), 269–280.
836 https://doi.org/10.1534/genetics.117.203380
837 Pedersen, B. S., & Quinlan, A. R. (2018). Mosdepth: Quick coverage calculation for genomes
838 and exomes. *Bioinformatics*, *34*(5), 867–868.
839 https://doi.org/10.1093/bioinformatics/btx699
840 Pietri, J. E., DeBruhl, H., & Sullivan, W. (2016). The rich somatic life of *Wolbachia*.
841 *MicrobiologyOpen*, *5*(6), 923–936. https://doi.org/10.1002/mbo3.390
842 Puterová, J., & Martínek, T. (2021). digIS: Towards detecting distant and putative novel
843 insertion sequence elements in prokaryotic genomes. *BMC Bioinformatics*, *22*(1),
844 258. https://doi.org/10.1186/s12859-021-04177-6
845 Qian, H., Qian, S., Zhang, J., & Kessler, M. (2024). Effects of climate and environmental
846 heterogeneity on the phylogenetic structure of regional angiosperm floras
847 worldwide. *Nature Communications*, *15*(1), 1079. https://doi.org/10.1038/s41467-
848 024-45155-9

R Core Team. (2022). *R: A language and environment for statistical computing.* [Computer software]. https://www.R-project.org/

Rainey, P. B., & Travisano, M. (1998). Adaptive radiation in a heterogeneous environment. *Nature*, *394*(6688), Article 6688. https://doi.org/10.1038/27900

Regoes, R. R., Nowak, M. A., & Bonhoeffer, S. (2000). Evolution of virulence in a heterogeneous host population. *Evolution*, *54*(1), 64–71. https://doi.org/10.1111/j.0014-3820.2000.tb00008.x

Rigaud, T., & Juchault, P. (1995). Success and failure of horizontal transfers of feminizing *Wolbachia* endosymbionts in woodlice. *Journal of Evolutionary Biology*, *8*(2), 249–255. https://doi.org/10.1046/j.1420-9101.1995.8020249.x

Robinson, J. T., Thorvaldsdóttir, H., Wenger, A. M., Zehir, A., & Mesirov, J. P. (2017). Variant review with the integrative genomics viewer. *Cancer Research*, *77*(21), e31–e34. https://doi.org/10.1158/0008-5472.CAN-17-0337

Ross, P. A., Robinson, K. L., Yang, Q., Callahan, A. G., Schmidt, T. L., Axford, J. K., Coquilleau, M. P., Staunton, K. M., Townsend, M., Ritchie, S. A., Lau, M.-J., Gu, X., & Hoffmann, A. A. (2022). A decade of stability for wMel *Wolbachia* in natural *Aedes aegypti* populations. *PLOS Pathogens*, *18*(2), e1010256. https://doi.org/10.1371/journal.ppat.1010256

Sanaei, E., Charlat, S., & Engelstädter, J. (2021). *Wolbachia* host shifts: Routes, mechanisms, constraints and evolutionary consequences. *Biological Reviews*, *96*(2), 433–453. https://doi.org/10.1111/brv.12663

Sicard, M., Chevalier, F., De Vlechouver, M., Bouchon, D., Grève, P., & Braquart-Varnier, C. (2010). Variations of immune parameters in terrestrial isopods: A matter of gender,

aging and *Wolbachia*. *Naturwissenschaften*, *97*(9), 819–826. https://doi.org/10.1007/s00114-010-0699-2

Sicard, M., Dittmer, J., Grève, P., Bouchon, D., & Braquart-Varnier, C. (2014). A host as an ecosystem: *Wolbachia* coping with environmental constraints. *Environmental Microbiology*, *16*(12), 3583–3607. https://doi.org/10.1111/1462-2920.12573

Stein, A., Gerstner, K., & Kreft, H. (2014). Environmental heterogeneity as a universal driver of species richness across taxa, biomes and spatial scales. *Ecology Letters*, *17*(7), 866–880. https://doi.org/10.1111/ele.12277

Stein, A., & Kreft, H. (2015). Terminology and quantification of environmental heterogeneity in species-richness research. *Biological Reviews of the Cambridge Philosophical Society*, *90*(3), 815–836. https://doi.org/10.1111/brv.12135

Strunov, A., & Kiseleva, E. (2016). *Drosophila melanogaster* brain invasion: Pathogenic *Wolbachia* in central nervous system of the fly. *Insect Science*, *23*(2), 253–264. https://doi.org/10.1111/1744-7917.12187

Tatusova, T., DiCuccio, M., Badretdin, A., Chetvernin, V., Nawrocki, E. P., Zaslavsky, L., Lomsadze, A., Pruitt, K. D., Borodovsky, M., & Ostell, J. (2016). NCBI prokaryotic genome annotation pipeline. *Nucleic Acids Research*, *44*(14), 6614–6624. https://doi.org/10.1093/nar/gkw569

Templé, N., & Richard, F.-J. (2015). Intra-cellular bacterial infections affect learning and memory capacities of an invertebrate. *Frontiers in Zoology*, *12*(1), 36. https://doi.org/10.1186/s12983-015-0129-6

Therneau, T. M., until 2009), T. L. (original S.->R port and R. maintainer, Elizabeth, A., & Cynthia, C. (2024). *survival: Survival Analysis* (Version 3.6-4) [Computer software]. https://cran.r-project.org/web/packages/survival/index.html

896 Trevail, A. M., Green, J. A., Bolton, M., Daunt, F., Harris, S. M., Miller, P. I., Newton, S., Owen,
897 E., Polton, J. A., Robertson, G., Sharples, J., & Patrick, S. C. (2021). Environmental
898 heterogeneity promotes individual specialisation in habitat selection in a widely
899 distributed seabird. *Journal of Animal Ecology*, *90*(12), 2875–2887.
900 https://doi.org/10.1111/1365-2656.13588
901 Trouche, B., Schrieke, H., Duron, O., Eren, A. M., & Reveillaud, J. (2024). *Wolbachia*
902 populations across organs of individual *Culex pipiens*: Highly conserved intra-
903 individual core pangenome with inter-individual polymorphisms. *ISME*
904 *Communications*, ycae078. https://doi.org/10.1093/ismeco/ycae078
905 Turelli, M., Cooper, B. S., Richardson, K. M., Ginsberg, P. S., Peckenpaugh, B., Antelope, C. X.,
906 Kim, K. J., May, M. R., Abrieux, A., Wilson, D. A., Bronski, M. J., Moore, B. R., Gao, J.-J.,
907 Eisen, M. B., Chiu, J. C., Conner, W. R., & Hoffmann, A. A. (2018). Rapid global spread
908 of wRi-like *Wolbachia* across multiple *Drosophila*. *Current Biology*, *28*(6), 963-971.e8.
909 https://doi.org/10.1016/j.cub.2018.02.015
910 van Houte, S., Padfield, D., Gómez, P., Luján, A. M., Brockhurst, M. A., Paterson, S., &
911 Buckling, A. (2021). Compost spatial heterogeneity promotes evolutionary
912 diversification of a bacterium. *Journal of Evolutionary Biology*, *34*(2), 246–255.
913 https://doi.org/10.1111/jeb.13722
914 Vasimuddin, Md., Misra, S., Li, H., & Aluru, S. (2019). Efficient architecture-aware
915 acceleration of BWA-MEM for multicore systems. *2019 IEEE International Parallel*
916 *and Distributed Processing Symposium (IPDPS)*, 314–324.
917 https://doi.org/10.1109/IPDPS.2019.00041

Wernegreen, J. J., & Wheeler, D. E. (2009). Remaining flexible in old alliances: Functional plasticity in constrained mutualisms. *DNA and Cell Biology*, *28*(8), 371–382. https://doi.org/10.1089/dna.2009.0872

Werren, J. H., Baldo, L., & Clark, M. E. (2008). *Wolbachia*: Master manipulators of invertebrate biology. *Nature Reviews Microbiology*, *6*(10), 741–751. https://doi.org/10.1038/nrmicro1969

White, P. S., Choi, A., Pandey, R., Menezes, A., Penley, M., Gibson, A. K., de Roode, J., & Morran, L. (2020). Host heterogeneity mitigates virulence evolution. *Biology Letters*, *16*(1), 20190744. https://doi.org/10.1098/rsbl.2019.0744

Wick, R. R., & Holt, K. E. (2022). Polypolish: Short-read polishing of long-read bacterial genome assemblies. *PLOS Computational Biology*, *18*(1), e1009802. https://doi.org/10.1371/journal.pcbi.1009802

Wishart, D. S., Han, S., Saha, S., Oler, E., Peters, H., Grant, J. R., Stothard, P., & Gautam, V. (2023). PHASTEST: Faster than PHASTER, better than PHAST. *Nucleic Acids Research*, *51*(W1), W443–W450. https://doi.org/10.1093/nar/gkad382

Xiao, Y., Dolan, P. T., Goldstein, E. F., Li, M., Farkov, M., Brodsky, L., & Andino, R. (2017). Poliovirus intrahost evolution is required to overcome tissue-specific innate immune responses. *Nature Communications*, *8*(1), Article 1. https://doi.org/10.1038/s41467-017-00354-5

Yang, Z., Liu, X., Zhou, M., Ai, D., Wang, G., Wang, Y., Chu, C., & Lundholm, J. T. (2015). The effect of environmental heterogeneity on species richness depends on community position along the environmental gradient. *Scientific Reports*, *5*(1), 15723. https://doi.org/10.1038/srep15723

Table 1. Nucleotide difference between *Wolbachia* from three tissues of naturally infected *Armadillidium vulgare*. HAEM: haemolymph, NC: nerve chain, OVA: ovaries. Nucl: Nucleotide, AA: amino acid; Arg: arginine, Gln: glutamine

Genome position	Individual	Tissue	Frequency	Type of change	Nucl. change	AA change	ORF effect	Gene name	Functional domains
1269492	F1_2015	NC	0	Substitution	C -> T	Arg340Gln	Missense variant	ABOJ95_001275	No recognized functional domain
		OVA	0						
	F2_2015	NC	0						
		OVA	0						
	F_1999	HAEM	0.466						
		NC	0.584						
		OVA	0.239						

Figure captions

Figure 1. Survival rate of *Armadillidium vulgare* following *Wolbachia* (*w*VulC) trans-infection. Effect of tissue origin of injected *Wolbachia* on mortality of recipient hosts monitored (**A**) every 10 days from day 0 to day 60 post-injection and (**B**) every 15-20 days from day 0 to day 200 post-injection. Solid lines: recipient hosts injected with crushed filtered tissue from animals naturally infected by *Wolbachia w*Vulc. Dotted lines: control individuals injected with crushed filtered tissue *from A. vulgare* not infected by *Wolbachia.* The three colours correspond to the tissue of origin of Wolbachia. Green: nerve chain, red: ovaries, blue: haemolymph

Figure 2. Infection dynamics of *Wolbachia* (*w*VulC) in *Armadillidium vulgare* from day 0 to day 60 post-injection. (**A**) *Wolbachia* loads in nerve chain (green), haemolymph (blue) and ovaries (red) of recipient hosts trans-infected by *Wolbachia*, all source tissue considered. (**B**) Influence of *Wolbachia* tissue origin on infection dynamics in tissue loads in recipient host, all recipient tissue considered. Green: nerve chain, red: ovaries, blue: haemolymph. Error bars correspond to the standard error. Infection dynamics not connected by the same letter are significantly different ($p < 0.05$).

Figure 3. *Wolbachia* (*w*VulC) load in *Armadillidium vulgare* tissues six months post-injection. The coloured boxplots illustrate the tissue origin of Wolbachia (green: nerve chain, red: ovaries, blue: haemolymph). However, the analysis did not reveal any significant effect of the tissue origin of the bacteria on the intensity of infection (RQ) in the recipient host tissues. Boxes above and below the medians (horizontal lines) show the first and third quartiles, respectively. Black diamonds represent the means. Levels not connected by the same letter are significantly different ($p < 0.05$).

Figure 4 *Wolbachia* (*w*VulC) load in tissues from naturally infected females (source line). *Wolbachia* load was measured in the haemolymph, nerve chain and ovaries of 15 females from the source line. The analysis showed that the bacterial load was lower in the haemolymph than in the ovaries and nerve chain. Boxes above and below the medians (horizontal lines) show the first and third quartiles, respectively. Black diamonds represent the means. Levels not connected by the same letter are significantly different ($p < 0.05$). Green: nerve chain, red: ovaries, blue: haemolymph.

Figure 5. Circos plot of the *w*VulC *Wolbachia* genome. Prophage-derived regions are indicated inside the genome ideogram (outer track), with their colour corresponding to the score attributed by PHASTEST (dark blue: intact, light blue: questionable). Ticks on the ideogram are separated by 10 kb intervals, and indicated values are in Mb. Predicted protein-coding genes are represented by grey rectangles (second track), and Insertion Sequence elements by black rectangles (third track). In the fourth track, the normalized read coverage for 5 kb adjacent windows (averaged over recipient individuals) is represented for the different resequenced tissues: ovaries (red), nerve chain (green) and haemolymph (blue). The black line corresponds to a mean normalized coverage of one, and grey lines are separated by 0.1 unit. Black triangle indicates the position of the detected variant and the bold letter (C and T) correspond to the two alleles.

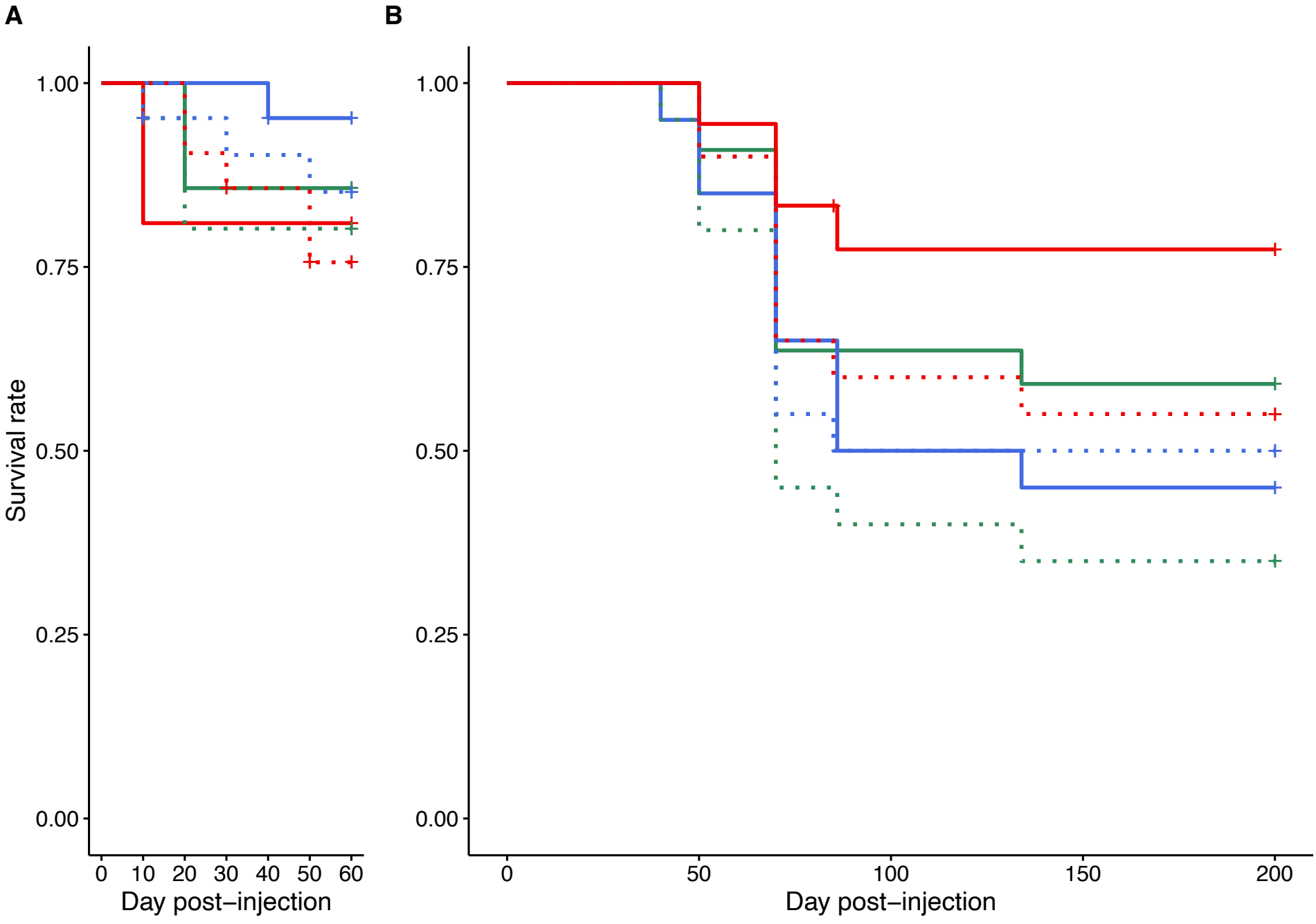
A
B
Survival rate
1.00
0.75
0.50
0.25
0.00
0
10
20
30
40
50
60
Day post−injection
0
50
100
150
200
Day post−injection

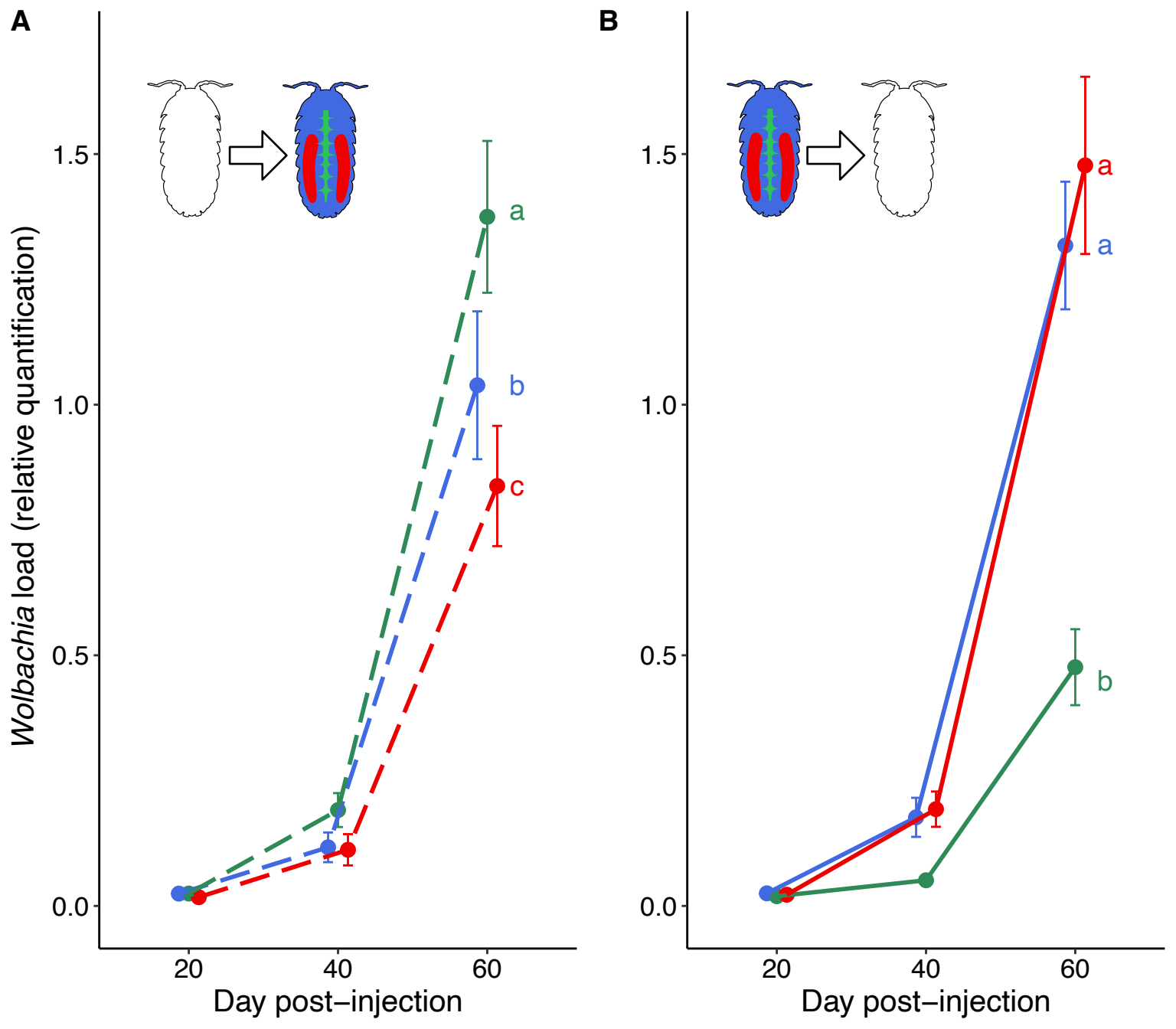
A
B
Wolbachia load (relative quantification)
1.5
1.0
0.5
0.0
20
40
60
Day post−injection
a
b
c
a
a
b

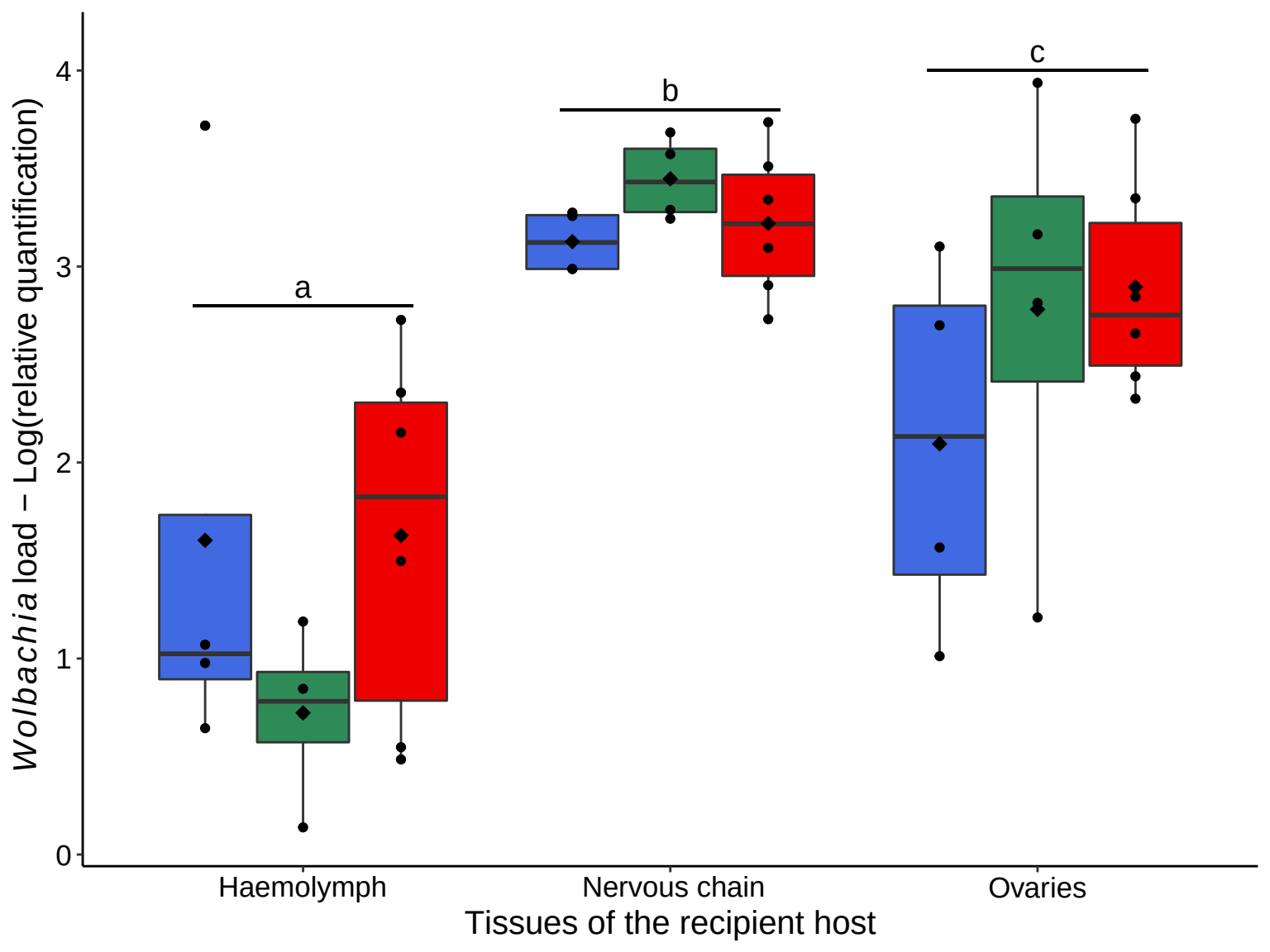
a
b
c
4
3
2
1
0
Wolbachia load – Log(relative quantification)
Haemolymph
Nervous chain
Ovaries
Tissues of the recipient host

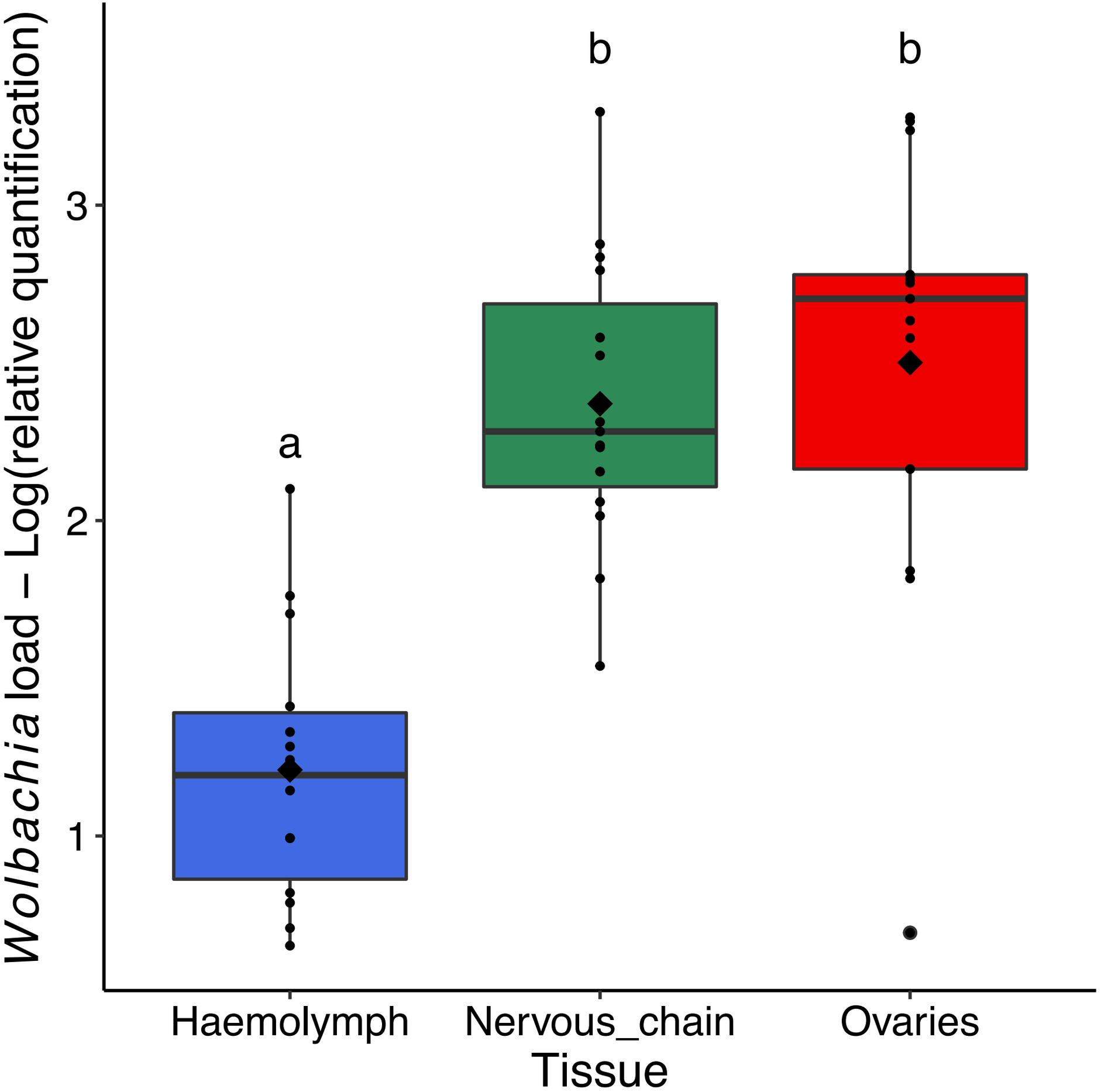
Wolbachia load – Log(relative quantification)
3
2
1
a
b
b
Haemolymph
Nervous_chain
Ovaries
Tissue

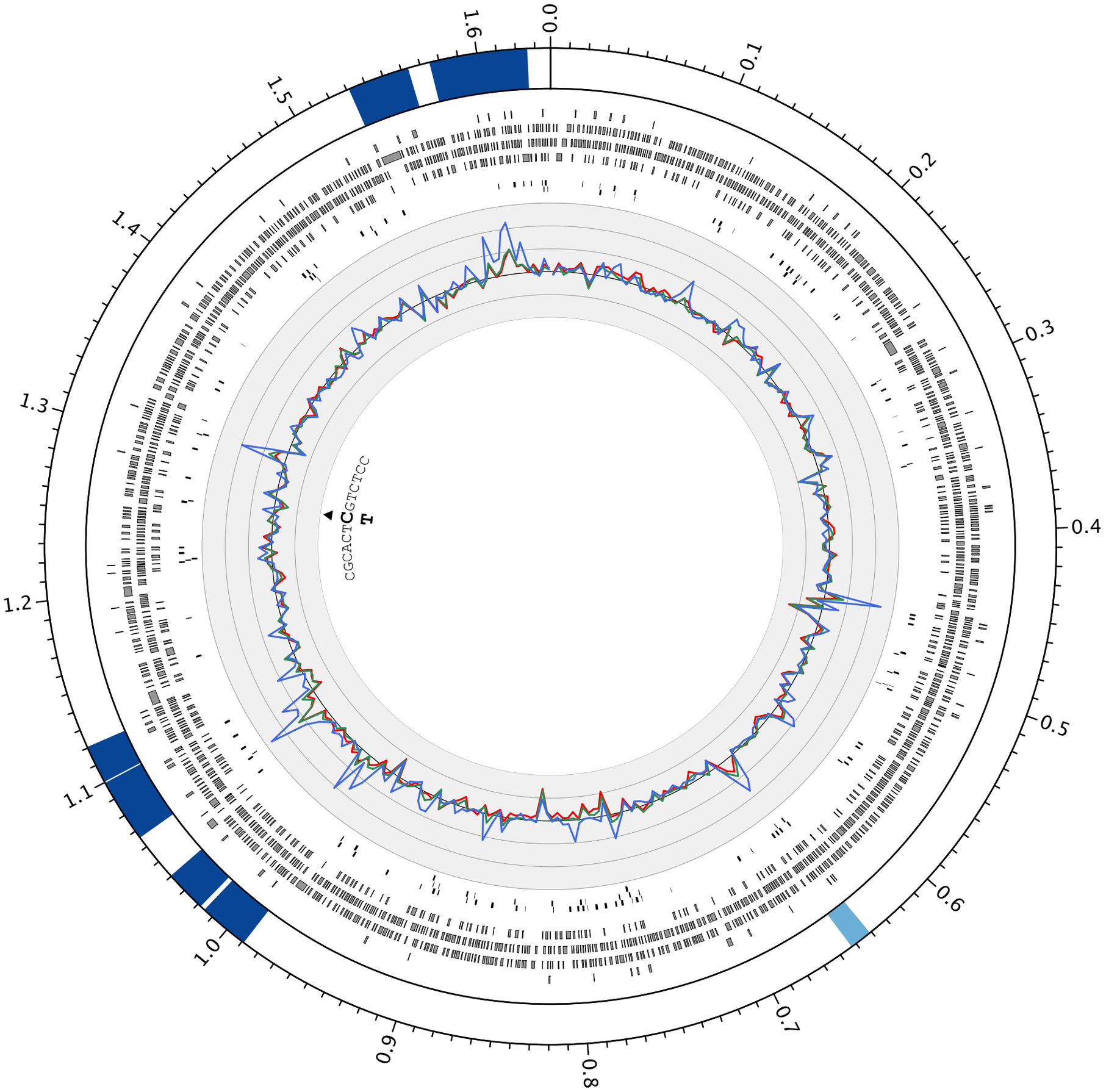
0.0
0.1
0.2
0.3
0.4
0.5
0.6
0.7
0.8
0.9
1.0
1.1
1.2
1.3
1.4
1.5
1.6
CGCACTCGTCTCC